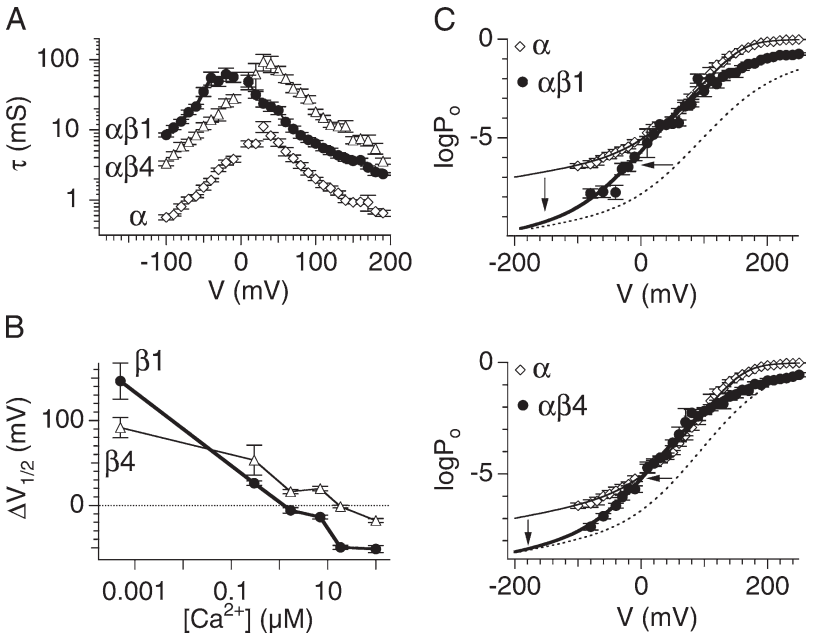

Figure S1. β1 and β4 share common gating effects. (A) Both β1 and β4 slow gating kinetics. Averaged activation and deactivation time constants at 7 μM Ca^{2+}. α, n = 10–13; αβ1, n = 13–27; αβ4, n = 12–26. (B) Both β1 and β4 increase steady-state opening at high Ca^{2+} but reduce opening in lower Ca^{2+}. $\Delta V_{1/2}$ represents differences between αβ channels and α alone channels. α, n = 8–44; αβ1, n = 7–39; αβ4, n = 10–26. (C) 0 Ca^{2+} $logP_o$-V relations reveal similar dual gating effects of β1 and β4: reducing intrinsic gating (downwards arrow) and stabilization of voltage sensor activation (leftwards arrow). These data have been reported in our previous publications (Wang and Brenner, 2006; Wang et al., 2006). α, n = 3–12; αβ1, n = 4–22; αβ4, n = 4–11. Error bars represent SEM.

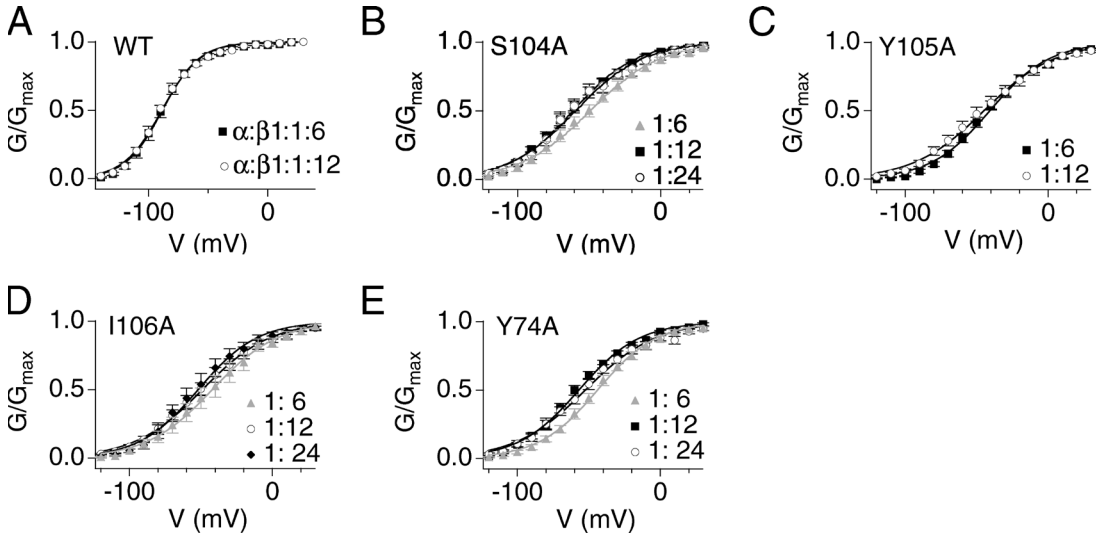

Figure S2. Alanine substitutions of four β1 residues alter G-V relations. (A–E) Averaged G-V relations of $\alpha\beta1_{WT}$, $\alpha\beta1_{S104A}$, $\alpha\beta1_{Y105A}$, $\alpha\beta1_{I106A}$, and $\alpha\beta1_{Y74A}$ at indicated α/β1 molar ratios. For $\alpha\beta1_{WT}$ and $\alpha\beta1_{Y105}$ channels, G-Vs largely overlap at both 1:6 and 1:12 α/β1 molar ratios, suggesting that β1 expression is saturated. For $\alpha\beta1_{S104A}$, $\alpha\beta1_{I106A}$, and $\alpha\beta1_{Y74A}$ channels, reducing α/β1 molar ratio from 1:6 to 1:12 caused negative G-V shifts; however, further reduction to 1:24 did not produce further negative G-V shifts. For the 1:12 α/β molar ratio, $\alpha\beta1_{WT}$, n = 14; $\alpha\beta1_{S104A}$, n = 9; $\alpha\beta1_{Y105A}$, n = 15; $\alpha\beta1_{I106A}$, n = 9; $\alpha\beta1_{Y74A}$, n = 14. For the 1:24 α/β1molar ratio, $\alpha\beta1_{S104A}$, n = 8; $\alpha\beta1_{I106A}$, n = 5; $\alpha\beta1_{Y74A}$, n = 10. Error bars represent SEM.

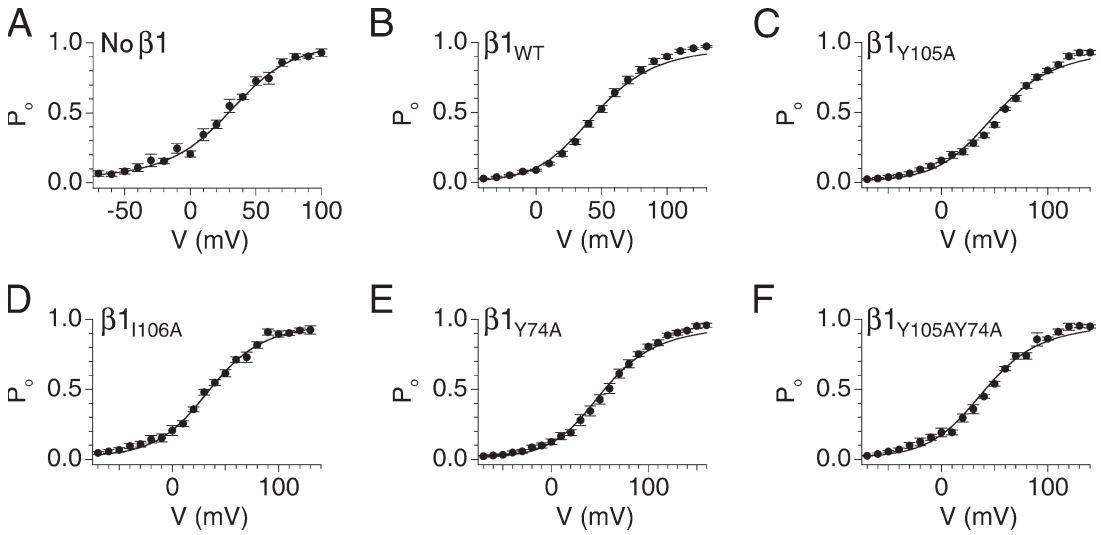

Figure S3. Segment A and B residues contribute to stabilization of open-channel voltage sensor activation. (A–F) Averaged P_o-V relations (circles) and best fits to the Horrigan-Aldrich model (black curves). The number of patches is the same as in Fig. 7. Error bars represent SEM.

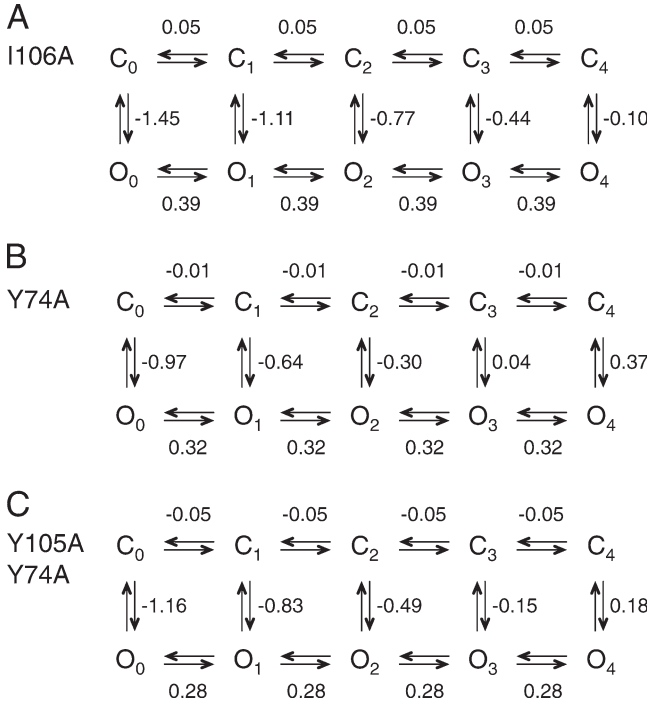

Figure S4. Effects of I106A, Y74A, and Y105AY74A on intrinsic gating and voltage sensor activation. Numbers indicate effects of the mutation on free energies associated with C-C transitions (right to left), O-O transitions (left to right), and C-O transitions (downward).

REFERENCES

Wang, B., and R. Brenner. 2006. An S6 mutation in BK channels reveals β1 subunit effects on intrinsic and voltage-dependent gating. *J. Gen. Physiol.* 128:731–744. http://dx.doi.org/10.1085/jgp.200609596

Wang, B., B.S. Rothberg, and R. Brenner. 2006. Mechanism of β4 subunit modulation of BK channels. *J. Gen. Physiol.* 127:449–465. http://dx.doi.org/10.1085/jgp.200509436